

# PHYSICAL REVIEW B

## SOLID STATE

THIRD SERIES, VOL. 2, NO. 10

15 NOVEMBER 1970

### Conductance Changes Produced by the Controlled Addition of Foreign Atoms to the Barrier of Al-Insulator-Metal Tunnel Junctions\*†

Paul Nielsen‡

*The James Franck Institute and Department of Physics, The University of Chicago, Chicago, Illinois 60637*

(Received 30 March 1970)

The conditions necessary for the occurrence of the two types of zero-bias conductance anomalies observed in certain tunnel junctions, (i) the large conductance dip ("giant resistance anomaly") and (ii) the small narrow conductance peak, were studied by introducing controlled amounts of impurities between the  $\text{Al}_2\text{O}_3$  barrier and the top electrode  $M$  of  $\text{Al}-\text{Al}_2\text{O}_3-M$  tunnel junctions. The elements Ti, Cr, Co, Cu, and their oxides, as well as CaO and Ge, were used in layer thicknesses up to  $30 \text{ \AA}$ . The effect of the dopant layer is dependent on the choice of Al or Ag for the metal  $M$ . This result is attributed to the different chemical reactivities of these metals. The small conductance peak treated by the theory of Appelbaum was found to occur only when unoxidized magnetic impurity was adjacent to the top electrode. Oxidized magnetic impurities, as well as CaO and Ge, produce a large conductance reduction. However, it was found that the reduction is very sharp for Ge and for partially reduced layers of the transition-metal oxides, but quite broad for CaO and well-oxidized transition metals. Although the conductance peak is associated with magnetic scattering, Appelbaum's theory does not account for the observed saturation of the peak at  $T \sim 1 \text{ K}$  as  $T$  is lowered. Reduction of the conductance peak by magnetic fields up to  $150 \text{ kG}$  yielded gyromagnetic ratios  $g = 1.50 \pm 0.15$  for Cr and  $g = 1.25 \pm 0.13$  for Ti. These values imply very strong exchange coupling of the magnetic dopants to the conduction electrons, in disagreement with the values predicted from the size and the saturation temperature of the conductance peak. The sharp conductance dip may be due to the fact that the partially reduced dopant layer forms an amorphous semiconductor and that tunneling occurs to a distribution of states which rapidly increases in density away from the Fermi level. The broad conductance reduction produced by well-oxidized dopants is attributed to the addition of a potential barrier  $> 0.5 \text{ eV}$  high to the  $\text{Al}_2\text{O}_3$  barrier.

#### I. INTRODUCTION

Electron tunneling through a thin insulating barrier between two normal metals has been studied extensively.<sup>1</sup> However, there are two types of zero-bias conductance anomalies which are still poorly understood, a small peak and a large conductance dip. Wyatt<sup>2</sup> found that the conductance of  $M-\text{MO}_x-\text{Al}$  junctions, where  $M$  was niobium or tantalum, shows a symmetrical peak at zero voltage with a half-width of a few mV. At  $4.2 \text{ K}$  the magnitude of the conductance peak is about 10% of the background conductance, and it increases logarithmically with decreasing temperature. Although initially explained as the result of a logarithmic density of states at the Fermi energy, Anderson<sup>3</sup> suggested magnetic scattering by surface states on the metal or magnetic impurities in the oxide as a more likely ex-

planation for this phenomenon. Appelbaum<sup>4,5</sup> calculated the effect of magnetic exchange interactions on electrons tunneling through a barrier containing magnetic impurities. Experiments by Shen and Rowell<sup>6</sup> showed satisfactory agreement with the temperature and magnetic field dependence of the conductance peak predicted by Appelbaum, but in their experiments the amount and kind of impurity was unknown. Moreover, an unexplained dependence of the magnitude of the peak on electrode material was observed.

A large conductance dip was later observed in  $M-\text{MO}_x-M$  junctions with a tunneling barrier of magnetic  $\text{Cr}_2\text{O}_3$  or  $\text{V}_2\text{O}_3$ .<sup>7</sup> In contrast with the small narrow conductance peak, this conductance dip is broader and orders of magnitude larger. The conductance was found to increase more or less linear-

ly with increasing bias, changing by several orders of magnitude in a few tens of mV. Although qualitatively different from the phenomenon explained by the Appelbaum theory, a calculation by Solyom and Zawadowski<sup>9</sup> showed that a conductance dip may also be caused by paramagnetic impurities located at one barrier-metal interface.

To determine whether these zero-bias effects are indeed due to magnetic interactions of tunneling electrons with impurities, it is necessary to add controlled amounts of magnetic and nonmagnetic atoms to the junction and to study the effect of these on the conductance curve. Investigations of Mezei<sup>9</sup> and Wyatt and Lythall<sup>10,11</sup> showed that chromium and titanium deliberately introduced onto an  $\text{Al}_2\text{O}_3$  barrier resulted in either a conductance peak or a conductance dip, depending on concentration. A later investigation of the effect of impurities, in which the amount and oxidation state was more precisely controlled,<sup>12</sup> indicated that deviations from the Appelbaum theory of the conductance peak occur when chromium is added and that the conductance dip is produced by oxidized chromium.

This paper describes the effects of controlled amounts of Ca, Ti, Cr, Co, Cu, their oxides, and Ge, deposited at the interface between the  $\text{Al}_2\text{O}_3$  barrier and the top metal electrode of Al- $\text{Al}_2\text{O}_3$ - $M$  tunnel junctions. In order to elucidate the dependence of the phenomena on the top electrode metal  $M$ , both aluminum and silver have been used. Because of the need for precise control of junction preparation and impurity deposition to obtain reproducible results, the methods employed are described in some detail in Sec. II. The effects of the oxidized dopants are considered in Sec. III; It is found that the cause of the sharp conductance dip is not magnetic scattering and various alternative mechanisms are discussed. In Sec. IV the conditions required for the production of the conductance peak are considered and the dependences on dopant thickness, temperature, voltage, and magnetic field are investigated.

## II. EXPERIMENTAL METHODS

### A. Preparation of Samples

The methods of junction preparation which were adopted had these primary objectives: (i) simultaneous deposition of different amounts of dopant onto six junctions with an identical barrier oxide in order to facilitate the comparison of different doping levels; (ii) control and determination of the relative and absolute amounts of dopant in the different junctions; (iii) fabrication of the junctions entirely in the controlled environment of a vacuum chamber so that the junctions would be reproducible from sample to sample and the composition of the barrier oxide unmodified by the contaminants in labora-

tory air.

The tunnel junctions were made in a system evacuated with a liquid-nitrogen-trapped oil diffusion pump. Provision was made for installing a mass spectrometer and ionization gauge close to the substrate position. The evaporant was resistance heated - chromium and titanium dopants were sublimed from bars of the metals. The total impurity content of the source materials was <10 ppm in Al, <100 ppm in Ag, <100 ppm in Ti, <100 ppm in Cr, and <1000 ppm in Co (mostly Fe and Ni).

Before a sample was made the system was baked to about 150 °C to remove much of the water film covering the inner surfaces. This bakeout was necessary to obtain reproducible junction impedances. After the chamber had cooled to about 25 °C the pressure was  $2 \times 10^{-7}$  Torr. A mass-spectrometer<sup>13</sup> analysis of the residual gases showed fractional amounts of about 0.65  $\text{H}_2\text{O}$ , 0.13  $\text{N}_2$ , and 0.20  $\text{H}_2$ , with traces of others. When aluminum was evaporated, the pressure rose to  $10^{-5}$  Torr due to the liberation of  $\text{H}_2$  from residual water films. The pressure rose to less than  $2 \times 10^{-6}$  Torr when other materials were evaporated, and in these cases also the pressure increase was found to be primarily due to  $\text{H}_2$ .

The samples were made on Pyrex glass substrates which had silver dots fired onto the surface along the edges. These silver dots provide solder points to which reliable low-temperature electrical contacts can be made. Before mounting a substrate in the vacuum system, the silver dots were polished and the Pyrex was cleaned with detergent in water, rinsed with distilled water, and blown dry with filtered air. Once the bakeout was completed, a wide aluminum strip was deposited on the glass to provide one electrode of the junctions. Two successive SiO evaporations through appropriate masks reduced the exposed metal surface to six square junction areas about  $0.3 \times 0.3$  mm and insulated the strip edges. After the aluminum strip had been oxidized different amounts of impurity atoms were deposited onto the junction areas, as discussed below, and the impurity layer could then be oxidized. Finally, six cross strips of aluminum or of silver were deposited to completely cover the junction areas, and a protective overcoat of SiO was applied. The aluminum, silver, and SiO layers had nominal thicknesses of 2000, 850, and 1200 Å, respectively. SiO-edge insulation was used to prevent the development of undesired structure in the conductance-voltage curves when the temperature was lowered below the superconducting transition temperature of the edges.<sup>14</sup> Samples were made with narrow electrode strips without edge insulation to assure that the junction region was not significantly modified by the spreading of SiO under the masks. Oxidation of the first aluminum strip, and of the im-

purity layer when desired, was accomplished by a plasma discharge<sup>15</sup> in 0.1 Torr of oxygen. The aluminum strip was oxidized for between 0.5 and 5 min, depending on the junction impedance desired, while 2 to 10 sec sufficed to oxidize the impurity layer.

#### B. Control of Film Thickness

A quartz-crystal deposition monitor<sup>16</sup> was used to determine the thickness of the various deposited films. The analog output of a frequency meter was recorded on a strip-chart recorder. A special shutter<sup>17</sup> was used to make possible deposition of a different amount of impurity atoms on each of the six junctions of a single sample. This shutter has a cutout sector with a different arc length for each junction. By rotating the cutout at constant speed past the sample, each junction was given a different known exposure. Combined with a known and constant deposition rate, the deposit thickness could then be calculated.

The accuracy of the thickness determination depends on a number of factors. First, it is well known<sup>18</sup> that the atoms incident on a surface may not all stick to it, and a substantial error could be introduced if the quartz crystal and the sample surface had different sticking coefficients. Because the same crystal was used to monitor all depositions, its surface was covered by the same material as that of the sample surface and incident atoms should have stuck equally well to both. This presumption was checked by exposing the crystal to evaporant after a constant evaporation rate had been established. It was found that the sticking coefficient did not change by more than 5% as the thickness increased from zero to several monolayers.

Second, the accuracy of the quartz-crystal deposition monitor itself must be known. Sauerbrey<sup>16</sup> and others<sup>19</sup> have found that, when temperature drifts are compensated and the entire vibrating part of the crystal is exposed to evaporant, the error is less than 1% of the amount calculated from

$$\Delta f = - (f^2 / \rho_Q N) \Delta m / A \quad (1)$$

which relates  $\Delta f$ , the frequency shift produced by the deposited mass per unit area  $\Delta m/A$ , to the initial crystal frequency  $f$ , the density of quartz  $\rho_Q$ , and the constant  $N = 167 \text{ kHz cm}$  for  $AT$ -cut crystals. The over-all calibration and measurement errors in  $\Delta f$  are estimated at  $\pm 0.02\Delta f \pm 0.3 \text{ Hz}$ , while the rate measurement obtained from the slope of  $\Delta f(t)$  has an error of about  $\pm 3\%$ . The uncertainties in the shutter openings are less than  $\pm 0.3\%$ , and thus the error in deposits made with the shutter is  $\pm 5\%$  of the amount deposited. Because the shutter alone determined the relative amounts deposited on different junctions of a sam-

ple, the error in these is less than  $\pm 1\%$ .

Third, the deposited mass per unit area has been converted to an equivalent thickness by using the bulk density of the layer. Although the actual thickness must be rough on an atomic scale, this equivalent thickness gives an average value. If the deposit consisted of isolated globules, such an average value would be of little interest; however, arguments against this possibility are discussed in detail in the Appendix. Moreover, the actual thickness may differ from that calculated because the density of the deposit or of oxidized deposit might differ from the bulk density, the deposit might consist in part of gas trapped during deposition, and the specific surface area of the  $\text{Al}_2\text{O}_3$  barrier might be greater than 1.0. There is no satisfactory way to investigate the density of the deposit in the thin dopant layers; however, it is unlikely to vary by more than 20% from the bulk values which were assumed. It is clear from previous work<sup>12</sup> that some gas must be trapped during deposition, but the amount appears small and has not been considered. Swaine and Plumb<sup>20</sup> have shown that the specific surface area of aluminum deposited at near normal incidence is 1.0. Because the  $\text{Al}_2\text{O}_3$  barrier layer grown on the aluminum must have the same specific surface area, the conversion of mass to thickness has been made assuming that the surface area is its geometrical value.

#### C. Measurements

The tunneling characteristics of the junctions were determined at temperatures below room temperature in a standard glass  $\text{He}^4$  Dewar or in an all metal  $\text{He}^3$  system.<sup>21</sup> The temperature was measured by means of a calibrated carbon resistor with an error of about  $\pm 1\%$ . When the temperature was below the superconducting transition temperature of aluminum, a solenoidal coil provided a magnetic field sufficient to suppress the superconductivity. Without the magnetic field the energy gap of the aluminum film was always apparent in the conductance-voltage curves of the junctions, and indicated that the conduction mechanism in the aluminum oxide was electron tunneling.

Standard ac modulation techniques were used to measure the differential conductance or resistance of the junctions. The  $p$ - $p$  ac voltage on the junction was kept less than or equal to  $kT$  to prevent modulation broadening. Because of this low modulation voltage the measurement accuracy was limited by thermal noise in the electronics - the error was  $\pm 0.2\%$  of the conductance. Absolute values of the conductance are accurate to a few percent. When the junction conductance was less than its capacitive reactance the current-voltage curve was measured and then differentiated numerically. In this case the error was between  $\pm 1\%$  and  $\pm 5\%$  of the conduc-

tance.

### III. LARGE CONDUCTANCE DIP

#### A. Experimental Results

A large and sharp conductance dip was observed when chromium<sup>9</sup> and titanium or copper<sup>10</sup> were placed in *M-I-M* junctions. However, the conditions of deposition caused partial oxidation of the metal dopant, and the oxidation state(s) responsible for the effect was not determined. Further studies<sup>12</sup> of the effect of chromium showed that the conductance dip resulted from oxidized or partially oxidized material. To completely investigate the relationship of the oxidation state to the appearance of a conductance dip it is also necessary to consider the effects of the electrode adjacent to the dopant. One might expect that a less electronegative metal would reduce or partly reduce the oxide of a more electronegative one. For example, the chromium-oxide layer might have been partly reduced by the aluminum electrode which was used in the previous experiments employing chromium as the dopant. Therefore, in these experiments a reactive metal, aluminum, and a noble metal, silver, were used as electrodes on otherwise identical

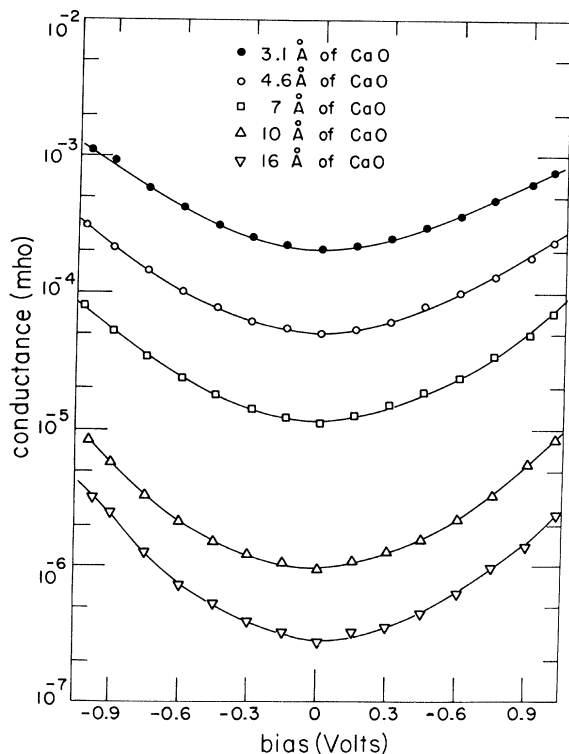


FIG. 1. Conductance-voltage curves of  $(\text{CaO}_x)\text{Al}$  junctions at 77°K. The conductance decreases by a few percent at 4.2°K.

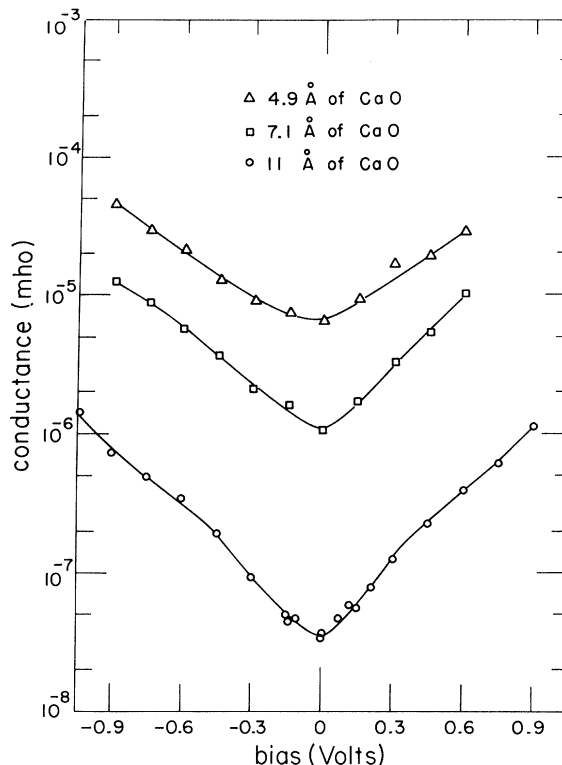


FIG. 2. Same as Fig. 1 for  $(\text{CaO}_x)\text{Ag}$  junctions.

junctions. To assure complete oxidation of the dopant prior to deposition of the electrode, the oxidation time was varied between 2 and 10 sec with no significant change in the effect of thin layers of dopant. In addition to determining the effect of dopant oxidation state, the hypothesis<sup>8</sup> that paramagnetic ions produce the sharp conductance dip was investigated. For this purpose a selection of dopant materials was made from the fourth period of the Periodic Table which included some elements with *d* electrons unpaired in any oxidation state and some which could be made paramagnetic or not by choice of the oxidation state.

Typical families of curves which result from adding different amounts of dopant to a single-barrier oxide of constant thickness are shown in Figs. 1-8 for oxides of calcium, titanium, chromium, and copper. The thickness of the oxide was calculated assuming the stoichiometric composition shown on each figure. Because the layer may be modified by the adjacent electrode the notation  $(\text{MO}_x)$  electrode is adopted for the completed junction.

Calcium oxide in  $(\text{CaO}_x)\text{Al}$  and  $(\text{CaO}_x)\text{Ag}$  junctions modifies the junction conductance in the way shown in Figs. 1 and 2. When the aluminum electrode is used the conductance is reduced by a factor which depends on the calcium oxide thickness, but is very

nearly independent of bias voltage. The shape of the  $G(V)$  curves on these semilog plots is, therefore, almost unchanged by the added calcium oxide. If a silver electrode is used instead of aluminum, the conductance curves do show some change in shape with increasing amount of calcium oxide, but the primary change is again a general reduction in the junction conductance. Increasing the measurement temperature from 4.2 to 300 °K increases the junction conductance by about 50%. At any temperature, equal thicknesses of calcium oxide in  $(\text{CaO}_x)\text{-Al}$  and  $(\text{CaO}_x)\text{-Ag}$  junctions reduce the conductance by very nearly equal factors.

Titanium oxide has an effect which depends on whether the structure is  $(\text{TiO}_x)\text{-Al}$  or  $(\text{TiO}_x)\text{-Ag}$ . Conductance curves for these two types are shown in Figs. 3 and 4. The reduction in conductance which is produced by the titanium oxide when it is covered with an aluminum electrode has the same shape and temperature dependence as that which has been observed<sup>10</sup> when partially oxidized titanium is covered with a silver electrode. At 4.2 °K and below, junctions which contain at least a monolayer of  $\text{TiO}_2$  have a zero-bias conductance minimum, shown in

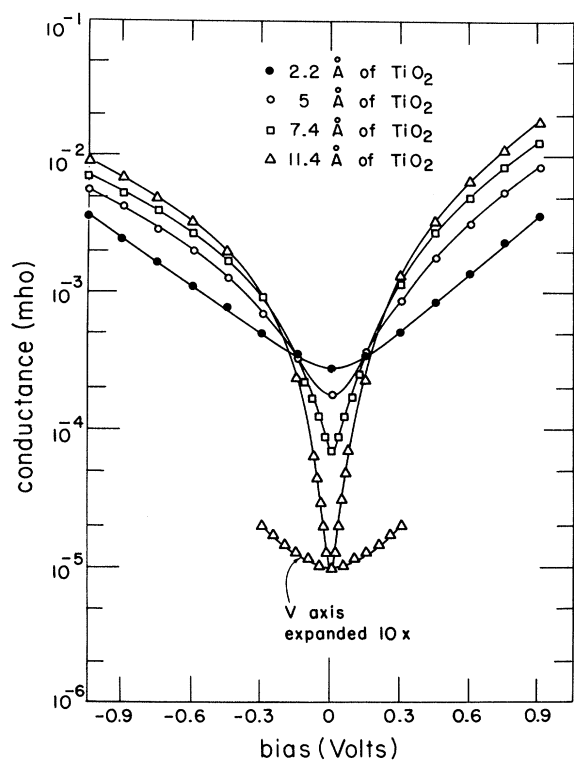


FIG. 3. Conductance-voltage curves of  $(\text{TiO}_x)\text{-Al}$  junctions. The zero-bias conductance peaks present at 2.2 and 5 Å of  $\text{TiO}_2$  are too small to be seen on the curves. The measurement temperature was 4.2 °K; reducing the temperature to 1.2 °K has no effect on the junction conductance.

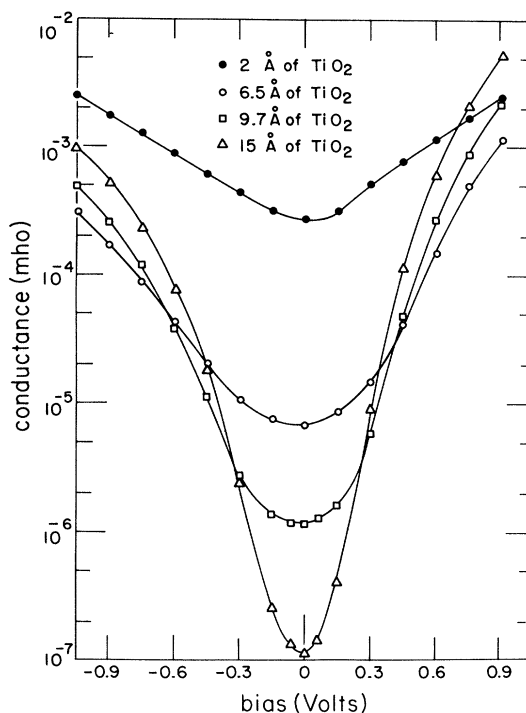


FIG. 4. Effect of layers of titanium oxide in junctions with a silver electrode. The curves were taken at 4.2 °K.

Fig. 3, which is as sharply pointed as the  $3.5kT$  broadening<sup>22</sup> produced by the temperature dependence of the Fermi distribution function permits. When the temperature is raised the minimum gradually becomes broader and shallower. For example, the zero-bias conductance of the junction doped with 11.4 Å of  $\text{TiO}_2$ , which is shown in Fig. 3, increases by a factor of 2 as the temperature is raised to 77 °K, and by another factor of 9 when the temperature is further increased to 300 °K. In contrast to  $(\text{TiO}_x)\text{-Al}$  junctions, the conductance reduction produced by titanium oxide covered with a silver electrode is very broad. The temperature dependence of the minimum is much less than in  $(\text{TiO}_x)\text{-Al}$  junctions with corresponding amounts of dopant; raising the temperature from 4.2 to 300 °K produces less than a factor of 2 increase in the conductance of junctions which contain less than 15 Å of  $\text{TiO}_2$ . However, the depth, sharpness, and temperature dependence of the minimum increase with increasing dopant thickness. This effect is already apparent in Fig. 4 where it can be seen that 15 Å of  $\text{TiO}_2$  produces a minimum considerably more pointed than does 9.7 Å. When 25 Å of titanium oxide is covered with a silver electrode, a sharp conductance dip, like that seen in  $(\text{TiO}_x)\text{-Al}$  junctions, is produced, and the zero-bias conductance at 4.2 °K is reduced by a factor of  $10^5$  below that of the undoped junction.

The effect of chromium oxide as a dopant in junc-

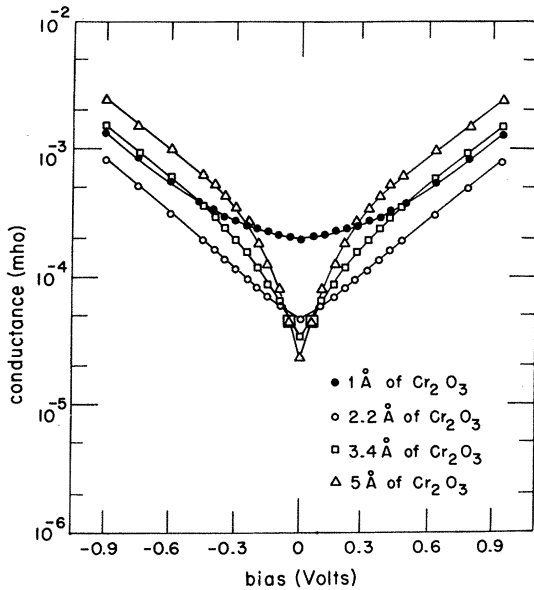


FIG. 5. Conductance-voltage curves at 4.2°K of  $(\text{CrO}_x)\text{-Al}$  junctions.

tions covered with aluminum and silver electrodes is shown in Figs. 5 and 6. The conductance-voltage curves show minima which are broader and more symmetrical than those produced by corresponding amounts of titanium oxide. However, we again see that the minima are sharply pointed when an aluminum electrode is used, but quite broad when

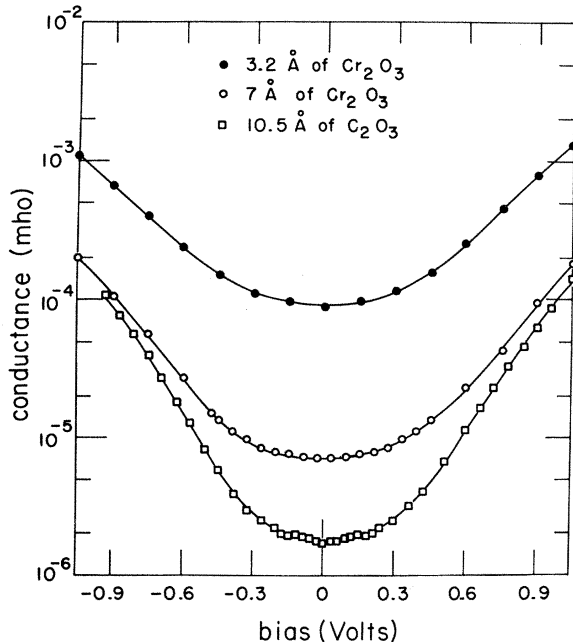


FIG. 6. Same as Fig. 4 for  $(\text{CrO}_x)\text{Ag}$  junctions.

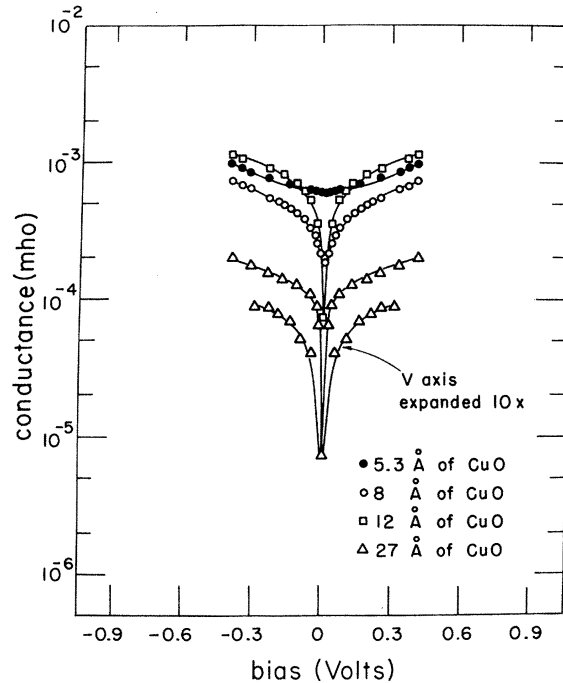


FIG. 7. Conductance-voltage curves of a series of  $(\text{CuO}_x)\text{Al}$  junctions. The extremely sharp dip at zero bias was measured at 1.17°K. At 4.2°K the zero-bias conductance of the junction containing 27 Å of CuO is about twice its value at 1.17°K, but this is consistent with the effect expected from thermal broadening of the Fermi distribution function.

a silver electrode covers the chromium oxide. The temperature dependence of the conductance of junctions doped with chromium oxide is like that of similar junctions doped with titanium oxide.

Figures 7 and 8 show the effect of copper oxide which is covered with an aluminum and a silver electrode. The general effect is similar to that produced by titanium or chromium oxides; however, the conductance dip of  $(\text{CuO}_x)\text{Al}$  junctions is narrower, while that of  $(\text{CuO}_x)\text{Ag}$  junctions is broader than those which appear in titanium- and chromium-oxide-doped junctions.

The modification to the conductance-voltage curves which results from adding a layer of transition-metal oxide to the tunnel junction depends strikingly on the adjacent electrode metal. A sharp dip in conductance at zero bias is produced by all these oxides when the electrode is aluminum, but a broad dip appears if silver is used instead. In contrast, the effect of calcium oxide is little influenced by the electrode metal.

For the sake of comparison, germanium was also deposited in thicknesses up to 31 Å and covered with aluminum and silver electrodes. A thickness of 27 Å covered with aluminum produces little change

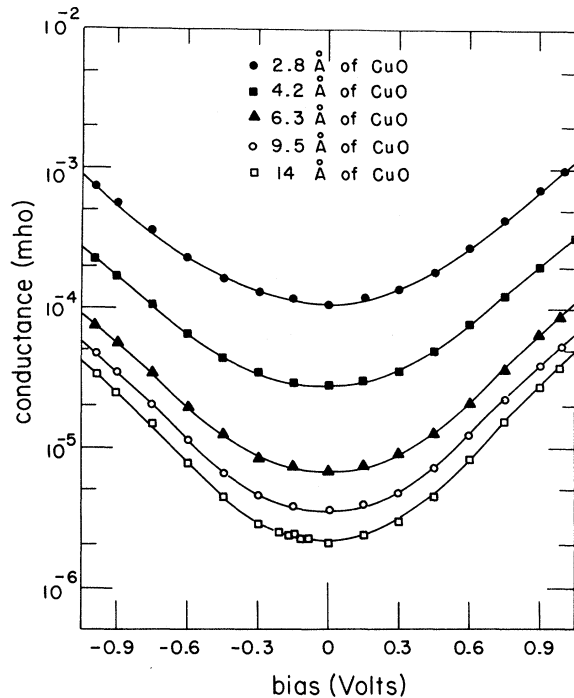


FIG. 8. Conductance-voltage curves for a series of  $(\text{CuO}_x)\text{Ag}$  junctions. In this case the effect of temperature variation over the range 4.2–77°K is negligible.

in the shape of  $G(V)$  and only a factor of 5 reduction in the zero-bias conductance. When 31 Å of germanium is covered with a silver electrode, the reduction in zero-bias conductance is a factor of 200. In this case, the shape of the conductance curve is the same as that of the curve in Fig. 3 for 7.4 Å of titanium oxide, but the width of the dip is about twice as large. Thinner layers of germanium in junctions with a silver electrode produce the rounded conductance dips typical of  $(\text{TiO}_x)\text{Ag}$  junctions.

## B. Discussion and Conclusions

### 1. Broad Conductance Reduction

Many investigations of the voltage dependence of the conductance of  $M-I-M$  junctions have shown that relatively simple barrier shapes suffice to explain the experimental observations.<sup>23</sup> The WKB approximation is used to obtain the tunneling probability and the prefactors to the exponential solution are generally omitted. Duke<sup>24</sup> has found that the conductance curve for a square barrier has a shape given by

$$G(V) \approx G(0) \cosh(V/2V_0), \quad (2)$$

where  $eV_0 = \phi/k\omega$ ,  $\phi$  = barrier height,  $\omega$  = barrier width, and  $k$  is given by  $k^2 = 2m_e\phi/\hbar^2$ . With a barrier 20 Å thick and 2 eV high, the conductance doubles in 0.3 V, in good agreement with the measured

behavior of these undoped and lightly doped junctions, and also with previous studies of  $\text{Al-I-Al}$  junctions.<sup>25</sup> Much more elaborate parametrizations of the conductance are possible,<sup>23</sup> but for the present purpose this square-barrier calculation is sufficient.

We have found that a broad conductance reduction is produced when metal oxides are placed on the aluminum oxide barrier and a covering electrode of silver is used. Because the stoichiometric metal oxides are insulators in bulk, it is reasonable to suppose that they form an additional tunneling barrier which causes this conductance reduction. An oversimplified model of the barrier, which nonetheless reproduces the principal features of the experimental curves, is illustrated in Fig. 9. At zero bias, the potential barriers of the  $\text{Al}_2\text{O}_3$  and the metal oxide are idealized as square barriers of

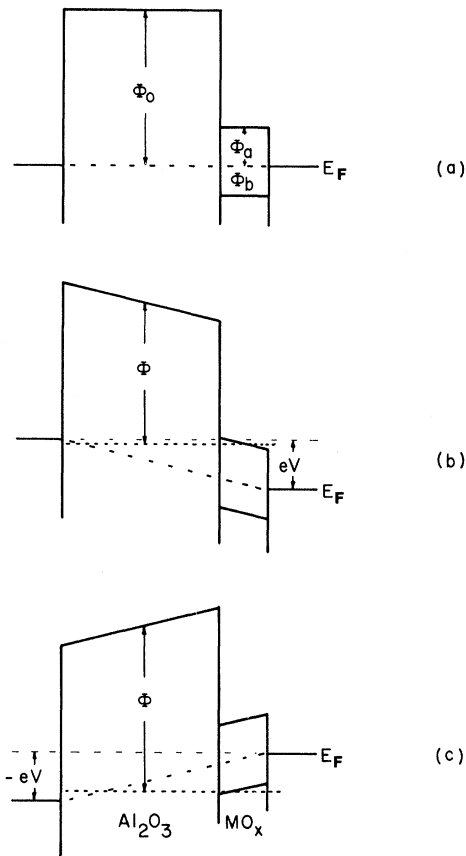


FIG. 9. An idealized potential barrier model for junctions with the structure  $(\text{MO}_x)\text{Ag}$ . In (a) is shown the barrier at zero bias together with the barrier height  $\phi_0$  of the  $\text{Al}_2\text{O}_3$  layer, the barrier height  $\phi_a$  of the  $\text{MO}_x$  layer, and the energy  $\phi_b$  by which the valence band of the  $\text{MO}_x$  layer lies below the Fermi energy. When a forward bias of  $eV$  is applied, this barrier is modified to the one shown at (b). The height of the barrier above one possible tunneling electron energy is indicated as  $\phi$ . A reverse bias of  $-eV$  changes the barrier to the one shown at (c).

TABLE I. Approximate barrier heights  $\phi_a$  and  $\phi'_a$  of different oxides covered with a silver electrode.  $\phi_a$  is estimated from the shape of the conductance curves and  $\phi'_a$  is calculated from the zero-bias conductance reduction produced by the oxides. Also shown are values of  $\frac{1}{2}E_g$  for the crystalline oxides.

Oxide	$\phi_a$	$\phi'_a$ at 1 Å	$\phi'_a$ at 15 Å	$\frac{1}{2}E_g$
CaO	~ 2 eV	0.8 eV	0.03 eV	> 2.8 eV <sup>a</sup>
TiO <sub>2</sub>	~ 0.5	1.6	0.09	1.5 <sup>b</sup>
Cr <sub>2</sub> O <sub>3</sub>	~ 0.8	0.5	0.2	1.7 <sup>c</sup>
CuO	~ 2	0.6	0	See text
Cu <sub>2</sub> O				1.0 <sup>b</sup>

<sup>a</sup>A. R. Hutson, in *Semiconductors*, edited by N. B. Hannay (Reinhold, New York, 1959), p. 577.

<sup>b</sup>R. H. Bube, *Photoconductivity of Solids* (Wiley, New York, 1969), p. 233.

<sup>c</sup>D. Adler, in *Solid State Physics*, Vol. 21, edited by F. Seitz, D. Turnbull, and H. Ehrenreich (Academic, New York, 1968), pp. 1-112.

heights  $\phi_0$  and  $\phi_a$ , respectively. In the forward direction of current flow (electrons going from the aluminum to the silver electrode) the height of the composite potential barrier is  $\phi$ , a function of the energy of the tunneling electron and of position in the barrier. The tunneling conductance can be calculated exactly by numerical methods, but it may be estimated from the probability for electrons to tunnel at the energy  $E_f + eV$ , ignoring the change in the tunneling probability of lower-energy electrons which results from the bias-produced change in the barrier shape. In this approximation, the effect of the added oxide barrier will become zero for an applied bias  $eV = (t+d)\phi_a/t$ , where  $t$  and  $d$  are the thickness of the Al<sub>2</sub>O<sub>3</sub> and the added oxide layer, respectively, since at this bias, electrons can tunnel directly to the conduction band of the oxide. Since the reverse bias conductance is nearly symmetrical to forward bias, it is also necessary to suppose that the valence band of the added oxide is at an energy  $-\phi_b$  below the Fermi level, where  $\phi_b \approx \phi_a$ . Then, when the junction is reversed-biased, electrons may tunnel from the valence band of the added oxide for  $eV \leq -(t+d)\phi_b/t$ . Without this tunneling path the asymmetrical barrier consisting of  $\phi_0$  and  $\phi_a$  alone would produce a strongly asymmetrical conductance-voltage curve.

If  $\phi_a \ll \phi_0$  so that the probability for tunneling through the Al<sub>2</sub>O<sub>3</sub> barrier is in fact constant over the bias range of interest, this model predicts that the  $G(V)$  curves for doped junctions should merge with the curve for an undoped junction at biases  $eV \approx \phi_a$  and  $-eV \approx -\phi_b$ . In the case of (TiO<sub>x</sub>)Ag junctions, the  $G(V)$  curves actually rise slightly above the conductance of a lightly doped junction for forward bias and remain below it for reverse bias. This is understandable since the Al<sub>2</sub>O<sub>3</sub> barrier will

actually reduce the tunneling probability more with reverse than forward bias.<sup>26</sup> The  $G(V)$  curves for the other oxides lie below the reference junctions at all biases, indicating that the added barrier is more nearly equal to the Al<sub>2</sub>O<sub>3</sub> barrier. Values of  $\phi_a$  estimated from these curves are given in Table I.

It is also possible to determine the barrier in another way. One assumes again that the additional oxide layer produces a square barrier, and then equates the reduction in the tunneling probability produced by such a barrier with the change in junction conductance which is observed at zero bias. The free-electron mass  $m$  and the thickness of stoichiometric oxide  $d$  are used in WKB tunneling-probability equation

$$P = \exp[-2d(2m\phi'_a)^{1/2}] \quad (3)$$

to determine this equivalent barrier height  $\phi'_a$ . The values so obtained are listed in Table I. The effective barrier height is about 1 eV when the barrier is 1 Å thick (as extrapolated from 3 to 5 Å barrier thicknesses). Because the relationship of the average barrier thickness to the tunneling thickness is probably different for the various oxides, as discussed below, it does not appear possible to relate the variations in effective barrier height to specific properties of the oxides, such as their polarizabilities. Bulk values of such properties could not be expected for layers less than one molecule thick, in any case.

The decrease in  $P$  upon the addition of 1 Å of oxide to a 15-Å layer determines the effective barrier height of the oxide at this thickness. The values of  $\phi'_a$  so obtained are very much less than the values of  $\phi_a$  determined from the  $G(V)$  curves. For both titanium and chromium oxides,  $\phi_a$  is about  $4\phi'_a$ , but in the case of calcium and copper oxides  $\phi'_a$  is close to zero although  $\phi_a$  must be greater than 1 eV. This difference between  $\phi_a$  and  $\phi'_a$  may be due to variations in the thickness of the added oxide which permit the thinner regions to contribute a large tunneling current although the barrier remains high. The surface roughness which must be assumed does not contradict the evidence for uniform layers that is discussed in the Appendix; furthermore, the fact that copper oxide produces the lowest effective barrier accords with the expectation that copper oxide layers should be the most granular.

The barrier heights found using this model are also compared in Table I with  $\frac{1}{2}$  of the energy gap of the crystalline solids. The values of  $\phi_a$  are consistently somewhat larger than  $\frac{1}{4}E_g$  in the cases of calcium, chromium, and titanium oxides. The reduction of  $\phi_a$  below  $\frac{1}{2}E_g$  is certainly the result of image force corrections to the barrier. It does not appear fruitful to include them in order to make a more exact comparison because  $E_g$  of the thin oxide



is likely to be somewhat different from the crystal-line-oxide energy gap. The energy gap of normally prepared CuO may be estimated from the color (black) and the activation energy for electrical conduction<sup>27</sup> to be about 1 eV, but this energy gap may not be that of a stoichiometric oxide. These measurements suggest that the oxide which is formed is CuO, since Cu<sub>2</sub>O with a 2-eV energy gap would have a different effect on the junction conductance, and that amorphous stoichiometric CuO has a large energy gap comparable to CaO.

## 2. Sharp Conductance Dip

The hypothesis that magnetic moments in the oxide, or magnetic oxides, cause the sharp conductance dip must be rejected since (CrO<sub>x</sub>)Ag and (CuO<sub>x</sub>)Ag junctions do not show such a dip. Whatever the oxidation state of the chromium, it will at least be paramagnetic and, as in the case of Cr<sub>2</sub>O<sub>3</sub>, it may be antiferromagnetic. The copper oxide may be either Cu<sub>2</sub>O or CuO. Thermal oxidation at high temperature produces Cu<sub>2</sub>O when the copper is a thin film on carbon.<sup>28</sup> In the strongly oxidizing plasma, CuO may be the more stable form, as it is on the metal at red-heat in oxygen; this is also suggested by the behavior of (CuO)Ag junctions. If the oxide is CuO and therefore paramagnetic, the flat  $G(V)$  curves of (CuO<sub>x</sub>)Ag junctions refute the association of magnetic oxides with the conductance dip. If it is Cu<sub>2</sub>O, on the other hand, neither the Cu<sup>+</sup> ions nor the mixture of Cu and Cu<sup>+</sup> ions in (CuO<sub>x</sub>)Al junctions have unpaired  $d$  electrons, and hence the paramagnetic impurity argument cannot explain the sharp conductance dip of (CuO<sub>x</sub>)Al junctions. The data for titanium oxide are inconclusive because TiO<sub>2</sub> is not paramagnetic while the (possibly) reduced oxide in (TiO<sub>x</sub>)Al junctions is. The calculation of Solom and Zawadowski,<sup>8</sup> which predicts a large conductance dip for paramagnetic impurities located within two atomic diameters of the electrode, should apply to both the thin layers in (CrO<sub>x</sub>)Ag and (CuO<sub>x</sub>)Ag junctions and to junctions containing unoxidized titanium, chromium, and cobalt (Sec. IV), but none of them shows this dip. The fact that the sharp conductance dip in (CrO<sub>x</sub>)Al and other junctions becomes increasingly deeper as the impurity-layer thickness increases also indicates that the dip is not explained by their calculation.

Christopher *et al.*<sup>29</sup> proposed that the sharp conductance dip in junctions with thick magnetic oxides could be due to a tunneling barrier only a few tens of meV high. This model is not applicable to barriers produced by a thin added layer because a much larger height is required to explain the value of the bias voltage at which the conductance curves of doped and undoped junctions merge and the magnitude of the zero-bias conductance reduction.

Graver and Zeller<sup>30</sup> have produced a sharp con-

ductance dip by imbedding in a tunneling barrier small metal particles which provide intermediate states for tunneling. However, the addition of metal particles to a barrier while maintaining the same total oxide thickness, as would occur if the aluminum electrode produced metal particles in the added oxide layer, cannot substantially reduce the junction conductance. Hence, tunneling through intermediate states of this sort cannot explain the observations.

The experimental results show that the aluminum electrode must be modifying the properties of the transition-metal oxides. The chemical stability of these oxides located at the interface between the Al<sub>2</sub>O<sub>3</sub> barrier and a silver or aluminum electrode may be estimated by calculating the bulk free-energy changes  $\Delta F$  which occur during the anticipated reactions.<sup>31</sup> One finds that all the metal oxides are stable next to silver electrode but that an aluminum electrode may reduce titanium, chromium, and copper oxides, with chromium oxide being the most stable. Measurements of the conductance peak produced by TiO<sub>2</sub>, which are discussed in Sec. IV, show that TiO<sub>2</sub> is reduced by the aluminum electrode. We conclude that added layers of all the oxides reducible by an aluminum electrode, as well as slowly deposited partially oxidized layers of transition-metal dopants, consist of an amorphous mixture of O<sup>2-</sup>, the transition metal in various oxidation states, aluminum ions, and possibly some aluminum.

The electrical properties of such an amorphous nonstoichiometric layer are even more difficult to understand than the properties of bulk amorphous semiconductors. However, models of amorphous semiconductors which suppose that it is mainly the local bonding which determines the properties should also be approximately correct for such very thin layers. One such model, which applies to alloy glasses, and which may therefore apply also to these oxide layers as they have been described above, is proposed by Cohen, Fritzsche, and Ovshinsky.<sup>32</sup> They suggest a band model in which the forbidden gap of a crystalline semiconductor is replaced by a mobility gap. Within this gap there is a high density of localized states which decreases toward the center. The Fermi level is located near the center of the gap, and the high density of localized states permits very little change of its position when a metal electrode is placed against the alloy. The potential barrier previously described (Fig. 9) is applicable to this model. However, when forward or reverse bias is applied there is a possibility of tunneling to empty or from filled localized states within the oxide, in addition to the normal tunneling through the oxide. The energy distribution of the density of localized states which is proposed<sup>32</sup> enables this additional tunneling current to contribute a rapidly

increasing current as the junction is biased. Because these states are localized, the argument<sup>33</sup> that densities of states are not reflected in the tunneling characteristic does not apply. The model thus explains the sharp zero-bias conductance dip which is observed.

Titanium oxide layers of thickness greater than 20 Å are likely to have a nonstoichiometric composition in the part of the layer adjacent to the Al<sub>2</sub>O<sub>3</sub> barrier because titanium oxide grown on the metal (like aluminum oxide grown on aluminum) produces a thin layer which stops increasing at about this thickness. Therefore, the conductance dip produced by thicker titanium oxide layers covered by a silver electrode can also be explained by this model. Although the model was not expected to apply to germanium, the results of tunneling into both thin and thick<sup>34</sup> layers of germanium can be explained in this same way.

#### IV. CONDUCTANCE PEAK

##### A. Theory

Appelbaum<sup>5</sup> has treated the effect of isolated magnetic impurities in the tunneling Hamiltonian formalism.<sup>35</sup> The parts of the Hamiltonian which result from electron spin-flip terms are included in the perturbation  $\mathcal{K}'$  and the transition rate is evaluated up to third order in  $\mathcal{K}'$ . The junction conductance in zero magnetic field is found to be

$$G(T, V) = G^{(2)} + G^{(3)}(T, V). \quad (4)$$

With a slight modification to Appelbaum's notation, the second-order term is

$$G^{(2)} = (4\pi e^2/\hbar)\rho\rho' \{T^2 + N[2TT_a + T_a^2 + S(S+1)T_j^2]\}, \quad (5)$$

and the third-order term which determines the conductance peak is

$$G^{(3)}(T, V) = [16\pi e^2 S(S+1)/\hbar]\rho\rho' N T_j^2 J F(eV). \quad (6)$$

$F(eV)$  must be numerically evaluated; however, it was approximated by

$$F(eV) = -\rho \ln [(|eV| + nkT)/E_0]. \quad (7)$$

$T$ ,  $T_a$ , and  $T_j$  are the tunneling matrix elements for electrons which do not interact with the paramagnetic impurities, which have nonexchange interactions, and which have exchange interactions, respectively.  $J$  is the exchange coupling between the conduction electrons and impurity of spin  $S$ .  $N$  is the area density of impurities.  $\rho$  and  $\rho'$  are the densities of states of electrons in the two electrodes, taken at the Fermi energies. The constant  $n$  is equal to 1.35.<sup>6</sup>  $E_0$  is an energy cutoff which must be introduced because  $\rho$ ,  $T_j$ , and  $J$  are assumed independent of energy – it could be determined if the energy dependences of these quantities

were known. Considering only  $\rho(\epsilon)$ , Appelbaum estimated  $E_0 \approx 100$  meV. This is at least five times the experimental value and thus indicates a need for theoretical consideration of the energy dependences of  $T_j$  and  $J$  as well.

It is apparent from Eq. (7) that this conductance peak increases logarithmically with decreasing bias voltage at zero temperature; the zero-bias magnitude of the conductance peak also increases logarithmically with decreasing temperature. At a finite temperature  $T$ , the conductance peak increases nearly logarithmically as the bias is decreased to  $eV \approx nkT$  and then saturates.

A magnetic field applied to the junction reduces  $G^{(2)}$  when  $-\Delta < eV < \Delta$  ( $\Delta = g\mu_B B$  is the Zeeman energy of the impurity) and splits  $G^{(3)}$  into two conductance peaks centered at  $eV = \pm \Delta$  (a third peak which remains at  $eV = 0$  is of negligible magnitude). However, examination of the equations which describe  $G^{(2)}$  and  $G^{(3)}$  when a magnetic field is applied reveals that most of the change in the conductance peak is due to the field dependence of  $G^{(2)}$ , if  $G^{(3)}$  is less than 40% of the  $T_j^2$  term of  $G^{(2)}$ , as assumed by Appelbaum.<sup>5</sup> Only if  $G^{(3)}$  were equal to or greater than  $G^{(2)}$  could one expect to observe the predicted splitting of the  $G^{(3)}$  peak, but the perturbation expansion would then be invalid. Shen and Rowell<sup>6</sup> found that the entire magnetic field dependence of their junctions could be explained using  $G^{(2)}$  alone.

A more accurate representation of  $F(eV)$  than Eq. (7) is<sup>36</sup>

$$F(eV) = -\rho \ln \{[(eV)^2 + (nkT)^2]^{1/2}/E_0\}. \quad (8)$$

The best value of  $n$  in this equation is 1.84. Either approximation suffices to describe the temperature and voltage dependence of the junctions investigated by Shen and Rowell.<sup>6</sup> However, neither predicts the saturation of  $G(0)$  as the temperature is lowered, which has been observed in junctions with deliberately added chromium.<sup>12</sup> The observed conductance peak  $\Delta G(V, T)$  of such junctions can be described by

$$\Delta G(T, V) = -A \ln \{[(eV)^2 + nkT)^2 + \gamma^2]^{1/2}/E_0\}, \quad (9)$$

which contains the additional parameter  $\gamma$ . This equation will be used to parametrize the experimental results.

##### B. Results

###### 1. Temperature, Voltage, and Dopant Concentration Dependence

It has already been seen that titanium and chromium atoms added to tunnel junctions produce a conductance peak.<sup>9,11,12</sup> Since this conductance peak, as well as the large conductance dip, is influenced by the electrode material, various electrode materials were compared. In Table II the occurrence

TABLE II. Occurrence and thickness dependence of the conductance peak.

Dopant	Electrode	Dopant thickness range for a conductance peak
Ti	Al	0.3 Å to >63 Å
TiO <sub>2</sub>	Al	0.5 Å to 5 Å
Ti	Ag	0.3 Å to >63 Å
TiO <sub>2</sub>	Ag	none
Cr	Al	0.1 to 3 Å
Cr <sub>2</sub> O <sub>3</sub>	Al	none
Cr and Cr <sub>2</sub> O <sub>3</sub>	Ag, Cu, and In	none
Co	Al	0.5 to 8 Å
CoO	Al	none
Co and CoO	Ag	none
Cu and CuO	Al and Ag	none

and dependence of the conductance peak on dopant thickness are summarized; Table III gives the parameters  $n$ ,  $\gamma$ , and  $E_0$ , which are used in Eq. (9) to describe the temperature and voltage dependence of the conductance peak that is produced.

The dependence of the conductance peak on dopant thickness is shown explicitly in Fig. 10 for (Ti)Al junctions. (Ti)Ag junctions have a conductance peak with similar thickness dependence, but the values of  $\gamma$  are twice as large for corresponding thicknesses of dopant. Curves showing the thickness dependence of chromium-doped junction have already been given.<sup>12</sup> The value of  $\gamma$  in this case is independent of thickness and more than twice as large as the values found for junctions doped with 1 Å or less of titanium. Cobalt dopant produces a conductance peak with a temperature dependence similar to that produced by equal thicknesses of titanium; however, the conductance peak is not present when more than 8 Å of cobalt is deposited. No conductance peak is produced by copper.

## 2. Magnetic Field Dependence

The effect of magnetic fields up to 150 kG on the conductance peak was determined for some junctions containing chromium and titanium dopants.<sup>37</sup> A typical family of curves is shown in Fig. 11 for a titanium-doped junction. The data do not satisfactorily fit the expression obtained by Shen<sup>6</sup> for the temperature-broadened  $G^{(2)}$  conductance reduction predicted by Appelbaum because the measured broadening is magnetic field dependent and the values of  $\Delta(B)$  extrapolate to a large Zeeman energy at zero field. Addition of the  $G^{(3)}(B)$  term obtained by Appelbaum would not change the fit appreciably. Consequently, a different method of analyzing the field dependence of the conductance peak, which was suggested by Losee and Wolf,<sup>38</sup> has been employed.

TABLE III. Values of  $n$ ,  $\gamma$ , and  $E_0$  which describe the conductance peak through the equation  $\Delta G(V, T) = -A \ln\{[(eV)^2 + (nkT)^2 + \gamma^2]^{1/2}/E_0\}$ .

Dopant	Sample electrode materials	Dopant thickness (Å)	$n$	$\gamma$ (meV)	$E_0$ (meV)
Ti	Al	0.46	2.0	0.16	21
Ti	Al	1.55	1.7	0.17	21
Ti	Al	3.8	1.8	0.28	24
Ti	Al	8.6	2.1	0.32	21
Ti	Ag	1.02	1.4	0.15	13
Ti	Ag	1.54	1.9	0.36	18
Ti	Ag	2.3	1.9	0.44	19
Cr	Al	0.35	2.1	0.42	19
Cr	Al	0.50	2.4	0.33	22
Cr	Al	0.75	2.1	0.32	20
Co	Al	1.7	1.4	0.14	18
Co	Al	2.5	1.6	0.18	20
Co	Al	3.8	2.1	0.29	20

They predict for the  $G^{(2)}$  term a field-dependent broadening

$$\Gamma = \pi(J\rho)^2 \Delta \quad (10)$$

and a measured gyromagnetic ratio

$$g = g_0 - |2J\rho|. \quad (11)$$

$J\rho$  is the same product of exchange coupling and density of states which is incorporated in the Appelbaum theory,  $g_0$  is the ion  $g$  factor in the absence of exchange coupling, and  $\Delta = g\mu_B B$ . According to their calculations, the  $G^{(3)}$  term is so broadened and reduced in amplitude when the junction is in a magnetic field of 50 kG or greater that it may be neglected. The position of the peak of  $dG(V)/dV$  in high magnetic fields determines  $\Delta$  and the half-width of this peak determines  $\Gamma$ .

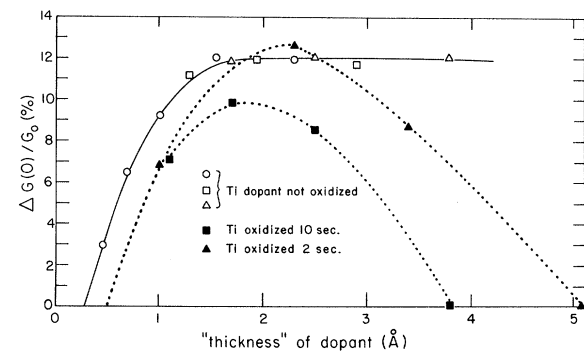


FIG. 10. Magnitude of the zero-bias conductance peak at 1.2 °K produced by titanium and titanium oxide covered with an aluminum layer. In all cases, the "thickness" is the value obtained from the bulk density of titanium.

Both the analysis of Appelbaum and that of Losee and Wolf assume that the magnetic impurities are independent of one another. However, experimental difficulties in determining  $dG(V)/dV$  for junctions with a small conductance peak necessitated the use of relatively large amounts of dopant to produce a large effect. Even then the errors in determining  $\Delta$  and  $\Gamma$  were rather large because  $dG(V)/dV$  could not be obtained electronically. In a (Cr)Al junction, 1.1 Å of chromium had  $g = 1.5 \pm 0.15$  while, determined from Eq. (9),  $J\rho = 0.4 \pm 0.06$ . In a (Ti)Al junction, 2.3 Å of titanium had  $g = 1.25 \pm 0.13$  and  $J\rho = 0.4 \pm 0.06$ . Similar values of  $g$  and  $J\rho$  were found with junctions containing somewhat smaller amounts of chromium or titanium, but the measurement error was larger.

### C. Discussion

Oxidation destroys the conductance peak in all except  $(\text{TiO}_x)\text{Al}$  junctions. Because  $\text{TiO}_2$  has no unpaired electron spins to produce an Appelbaum conductance peak, we conclude that some of the  $\text{TiO}_2$  is reduced by the Al electrode, as was assumed in Sec. III B 2. In every case, the first dopant atoms to

arrive at the  $\text{Al}_2\text{O}_3$  barrier are ineffective in producing a conductance peak. Because oxidation destroys the conductance peak, it appears that these first atoms react with excess oxygen left on the barrier after oxidation of the aluminum electrode.

The disappearance of the conductance peak upon oxidation, and the absence of a conductance peak in (Cr)Ag and (Co)Ag junctions, imply that the dopant can produce a conductance peak only when it is able to easily exchange electrons with the adjacent electrode. When unoxidized, the dopant will be bound to the aluminum electrode by bonds which are at least partially covalent<sup>39</sup> and thus involve the continuous exchange of electrons between dopant and electrode. But, when the dopant is oxidized, approximate charge neutrality at the interface requires that the negatively charged oxygen ions reduce the number of electrons on metal atoms in the vicinity – on dopant atoms primarily – thus reducing the number of valence electrons available for exchange between dopant and electrode. Furthermore, transition-metal–oxygen bonds are about 50% covalent,<sup>40</sup> and this covalent bonding within the oxidized dopant will further reduce the possibility of electron exchange between dopant atoms and electrode metal. The approximate monolayer of  $\text{H}_2\text{O}$  (or possibly<sup>41</sup> OH) chemisorbed on the dopant before the electrode was deposited will be destroyed when the aluminum electrode is evaporated, but the chemisorption energy is too large for it to be removed by the silver electrode.<sup>42</sup> Thus the absence of a conductance peak in (Cr)Ag and (Co)Ag junctions also leads to the conclusion that the dopant must be able to exchange electrons easily with the electrode to produce a conductance peak. The displacement by the silver electrode of the water on titanium dopant is somewhat puzzling since the chemisorption energy is probably higher than in the case of chromium or cobalt.<sup>42</sup> However, it may perhaps be explained by the easy reduction of  $\text{Ti}^{4+}$  to a mixture of lower oxidation states, which also accounts for the large negative free-energy change when  $\text{TiO}_2$  is reduced by aluminum and the consequent production of a conductance peak in  $(\text{TiO}_x)\text{Al}$  junctions. No surface studies adequate to substantiate this suggestion are known.

It has been recently predicted<sup>43</sup> that the dopant must be within a few atomic radii of the electrode to produce an appreciable conductance peak. The calculation does not take into consideration the atomic structure of the barrier and so cannot directly explain the effects of oxidation. However, its basic prediction is that the density of electrode electrons must be high at the position of the impurity, and the above discussion shows that this will not be the case when the dopant is oxidized.

Magnetic ordering which prevents free exchange of electron and impurity spin moments was pro-

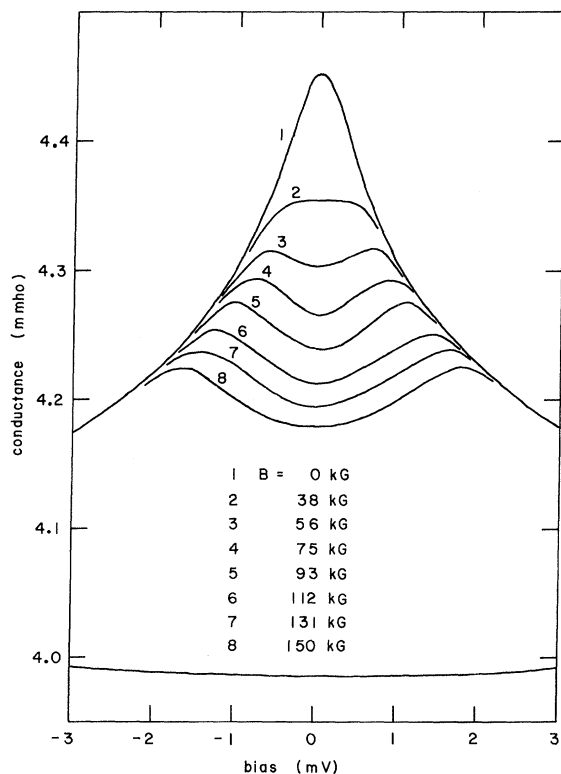


FIG. 11. Central portion of the conductance peak produced by 2.3 Å of titanium in a (Ti)Al junction at 1.3°K. The top curve was obtained at zero magnetic field and the seven curves below it at the successively higher fields indicated. The almost straight curve at the bottom is the background conductance of this junction.

posed<sup>12</sup> to explain the disappearance of the conductance peak produced by chromium when the dopant layer was thicker than 3 Å. The cobalt-dopant layers may be expected to order magnetically while titanium layers will not. Thus the persistence of the conductance peak with thick titanium layers and its absence beyond a thickness of 6–8 Å of cobalt appear to confirm this explanation. The hypothesis that magnetic ordering destroys the conductance peak is substantiated by the thickness required for the development of ferromagnetism in other thin magnetic films. For example, it has been found that films of iron become magnetically ordered upon adding the third monolayer of iron,<sup>44</sup> and that nickel layers become ferromagnetic at a thickness of about 3 Å.<sup>45</sup>

Analysis of the effect of high magnetic fields on the conductance peak produced by titanium and chromium gave  $J\rho = 0.4 \pm 0.06$  for both metals. Since the  $g$  values of both elements are likely to become almost 2.0 in a lattice,<sup>46</sup> this value of  $J\rho$  is consistent with the values of  $J\rho = 0.38 \pm 0.07$  for titanium and  $J\rho = 0.25 \pm 0.08$  for chromium which are obtained from Eq. (11) by assuming  $g_0 = 2.0$ . Similar values of  $J\rho$ , although much larger than  $J\rho \leq 0.1$  which is expected from data on the bulk Kondo effect, must also be assumed to explain the reduction in  $g$  from 2 which has been observed by others.<sup>6,11,47</sup> A saturation temperature may be obtained from  $J\rho$  by means of the equation<sup>48</sup>

$$kT_k \approx E_0 e^{-1/2J\rho}. \quad (12)$$

Below this temperature the strong coupling solution for the electron-impurity system<sup>48</sup> is expected to apply. The temperature obtained from this equation is about six times that of the experimental saturation temperature ( $\approx \gamma/nk$ ) for chromium; however, the error is large because of the exponential dependence on  $J\rho$  and the result might be accepted as an explanation of  $\gamma$  in this case. Unfortunately, the discrepancy is even larger for titanium, and in other experiments<sup>6,11,47</sup> where no saturation was observed. Furthermore, the experimental values of  $J\rho$  cannot be reconciled with the predicted magnitude<sup>48</sup> of the conductance peak in the strong coupling limit. Thus it does not appear possible to relate  $\gamma$  and  $J\rho$  by this calculation. The large values of  $J\rho$  required by the magnetic field measurements in this work and others<sup>6,11,47</sup> remain puzzling, not only because they are much larger than expected from Kondo-effect measurements, but also because they result in  $G^{(3)} \gg G^{(2)}$  and thus require a breakdown of the perturbation calculation.

## V. CONCLUSION

Three types of zero-bias conductance effects are produced by dopant layers in Al-Al<sub>2</sub>O<sub>3</sub>-M tunnel junctions. The large sharp conductance dip, pre-

viously attributed to magnetic scattering in the dopant, is explained by the electronic density of states in the amorphous nonstoichiometric layer. A large broad conductance reduction produced by well-oxidized dopant is apparently due to the tunneling barrier which the dopant layer adds to the Al<sub>2</sub>O<sub>3</sub> barrier. The small conductance peak discussed by Appelbaum is found to occur only when the paramagnetic dopant atoms are able to freely exchange electrons with the adjacent electrode. The observed saturation of the conductance peak with decreasing temperature has been described by an empirical constant which, however, cannot be related to the measured exchange coupling by the strong coupling theory.

## ACKNOWLEDGMENTS

I wish to thank D. L. Losee and E. L. Wolf for several valuable discussions about the theory of the  $g$  shift as well as for the measurement of the high-field conductance of some titanium- and chromium-doped junctions. I would also like to thank W. J. Brinkman for a discussion which clarified several points in the Appelbaum and Brinkman-Appelbaum calculations. I am particularly indebted to H. Fritzsche who first suggested this problem, and for his encouragement and guidance during its investigation.

The use of the facilities and the technical assistance of the personnel of the Low Temperature Laboratory and the Materials Preparation Laboratory of The James Franck Institute are gratefully acknowledged. Equipment used in this work was made available to The James Franck Institute of The University of Chicago by an ARPA grant.

## APPENDIX: CONTINUITY OF THE DEPOSIT

The observed large reductions of the junction conductance at zero bias which are produced by thin layers of oxidized dopant imply a rather complete and uniform coverage of the Al<sub>2</sub>O<sub>3</sub> barrier by the deposited dopant metal. Any bare patches between dopant clusters will add to the total junction conductance a conductance equal to that of an undoped junction of the same area. A layer of oxide (say CrO<sub>x</sub>) reduces the conductance by a factor of 10 at a thickness of 3.5 Å, and by a factor of 100 at 6 Å. If the barrier were infinitely high, the fractional coverages would have to be at least 0.9 and 0.99 for these two thicknesses. Since some electrons tunnel through the added layers, the actual coverage must be even more complete.

Independent evidence for these coverage factors would be desirable, but no *in situ* electron-microscope studies of deposition onto Al<sub>2</sub>O<sub>3</sub> layers appear to have been made. However, Neugebauer<sup>45</sup> and Gradman and Müller<sup>49</sup> deposited Ni onto glass at room temperature and NiFe onto copper, respec-

tively; they believe from both the magnetic properties and electron-microscope examination that films a few monolayers thick are continuous, with little or no island formation. Neugebauer's conditions are quite similar to deposition onto  $\text{Al}_2\text{O}_3$ , and the similarity of cobalt to nickel suggests that it should deposit in films with the same general structure. Titanium deposited on mica at 500–600 °C forms a continuous film at a thickness of less than 200 Å.<sup>50</sup> At 25 °C one would, therefore, not expect appreciable clustering. Relatively thick films of chromium have been examined by electron microscopy.<sup>51</sup> When the substrate temperature was below 450 °C, a very disordered structure was produced. This result indicates that little migration occurs and hence that

islands, if formed, remain only a few atoms in size. Copper has been deposited on carbon in high vacuum and subjected to various heat treatments and oxidation.<sup>28</sup> At an average thickness of 15 Å, the copper and copper oxide cover less than  $\frac{1}{3}$  of the total surface. However, the film was heated to 350 °C and oxidized in room air so there is some doubt about the structure of the freshly deposited film. General consideration of the nucleation of films<sup>52</sup> also shows that calcium, titanium, chromium, and cobalt should be quite immobile due to their high affinity for oxygen and relatively high melting temperatures, while copper is more likely to form clusters.

\*Research sponsored by the Air Force Office of Scientific Research, Office of Aerospace Research, USAF, under Contract No. AFOSR 49(638)-1653. The United States Government is authorized to reproduce and distribute reprints for governmental purposes notwithstanding any copyright notation hereon.

†Submitted in partial fulfillment of the requirements for the Ph.D. degree at the University of Chicago.

‡Fannie and John Hertz Foundation Fellow. Present address: Xerox Corporation, Rochester, N. Y. 14603.

<sup>1</sup>*Tunneling Phenomena in Solids*, edited by E. Burstein and S. Lundquist (Plenum, New York, 1969).

<sup>2</sup>A. F. G. Wyatt, Phys. Rev. Letters **13**, 401 (1964).

<sup>3</sup>P. W. Anderson (private communication to J. C. Phillips).

<sup>4</sup>J. Appelbaum, Phys. Rev. Letters **17**, 91 (1966).

<sup>5</sup>J. Appelbaum, Phys. Rev. **154**, 633 (1967).

<sup>6</sup>L. Y. L. Shen and J. M. Rowell, Phys. Rev. **165**, 566 (1968).

<sup>7</sup>L. Y. L. Shen and J. M. Rowell, Solid State Commun. **5**, 189 (1967).

<sup>8</sup>J. Solyom and A. Zawadowski, Physik Kondensierten Materie **7**, 325 (1968); **7**, 342 (1968).

<sup>9</sup>P. Mezei, Phys. Letters **25A**, 534 (1967).

<sup>10</sup>A. F. G. Wyatt and D. J. Lythall, Phys. Letters **25A**, 541 (1967).

<sup>11</sup>D. J. Lythall and A. F. G. Wyatt, Phys. Rev. Letters **20**, 1361 (1968).

<sup>12</sup>P. Nielsen, Solid State Commun. **7**, 1429 (1969).

<sup>13</sup>Model MS 10, manufactured by AEI, Ltd., England.

<sup>14</sup>T. Halpern and P. Nielsen, Bull. Am. Phys. Soc. **13**, 475 (1968).

<sup>15</sup>S. R. Pollack (private communication); see also J. H. Miles and P. H. Smith, J. Electrochem. Soc. **110**, 1240 (1963).

<sup>16</sup>G. Sauerbrey, Z. Physik **155**, 206 (1959).

<sup>17</sup>H. Fritzsche and P. Nielsen (unpublished).

<sup>18</sup>S. Dushman, *Scientific Foundations of Vacuum Technique* (Wiley, New York, 1962), 2nd ed., pp. 18, 408.

<sup>19</sup>One recent study is R. M. Mueller and W. White, Rev. Sci. Instr. **39**, 291 (1968).

<sup>20</sup>J. W. Swaine, Jr. and R. C. Plumb, J. Appl. Phys. **33**, 2378 (1962).

<sup>21</sup>T. Halpern and H. Fritzsche, Rev. Sci. Instr. **39**, 1336 (1968).

<sup>22</sup>S. Bermon and D. M. Ginsberg, Phys. Rev. **135**, A306 (1964).

<sup>23</sup>C. B. Duke, *Tunneling in Solids* (Academic, New York, 1969).

<sup>24</sup>Ref. 1, p. 43.

<sup>25</sup>For example, S. R. Pollack and C. E. Morris, Trans. Met. Soc. AIME **233**, 497 (1965).

<sup>26</sup>The slight rise in conductance above that of an undoped junction may be due to electrode effects similar to those discussed by R. M. Handy, Phys. Rev. **126**, 1968 (1962).

<sup>27</sup>I. T. Sheftel', A. I. Zaslavskii, E. V. Kurlina, and G. N. Tekster-Proskuryakova, Fiz. Tverd. Tela [Soviet Phys. Solid State **1**, 203 (1959)].

<sup>28</sup>B. M. Siegal and C. C. Peterson, in *Structure and Properties of Thin Films*, edited by C. A. Neugebauer, J. B. Newkirk, and D. A. Vermilyea (Wiley, New York, 1959), pp. 97–107.

<sup>29</sup>J. E. Christopher, R. V. Coleman, A. Isin, and R. C. Morris, Phys. Rev. **172**, 485 (1968).

<sup>30</sup>I. Giaever and H. R. Zeller, Phys. Rev. Letters **20**, 1504 (1968).

<sup>31</sup>F. D. Rossini, D. D. Wagman, W. H. Evans, S. Levine, and I. Joffe, *Selected Values of Chemical Thermodynamic Properties*, Circular No. 500 of the U. S. National Bureau of Standards, (U. S. Dept. of Commerce, Washington, D. C., 1952).

<sup>32</sup>M. H. Cohen, H. Fritzsche, and S. R. Ovshinsky, Phys. Rev. Letters **22**, 1065 (1969).

<sup>33</sup>W. A. Harrison, Phys. Rev. **123**, 85 (1961).

<sup>34</sup>The difference between (Ge)Al and (Ge)Ag junctions with a thin germanium layer is certainly due to the large solubility of aluminum, and the small solubility of silver, in germanium at room temperature [F. A. Trumbore, Bell System Tech. J. **39**, 205 (1960)]. The effects of thick layers of germanium have been discussed by J. W. Osmun and H. Fritzsche, Appl. Phys. Letters **16**, 87 (1970).

<sup>35</sup>M. H. Cohen, L. M. Falicov, and J. C. Phillips, Phys. Rev. Letters **8**, 316 (1962).

<sup>36</sup>E. L. Wolf and D. L. Losee (private communication).

<sup>37</sup>These measurements were made at the Francis Bitter National Magnet Laboratory by E. L. Wolf and D. L. Losee.

<sup>38</sup>E. L. Wolf and D. L. Losee, Phys. Rev. B **2**, 3670 (1970).

<sup>39</sup>J. D. Levine and E. P. Gyftopoulos, Surface Sci. **1**, 171 (1964).

<sup>40</sup>L. Pauling, *General Chemistry* (Freeman, San Francisco, 1959), 2nd ed., p. 235.

<sup>41</sup>S. J. Gregg, in *Chemisorption*, edited by W. E. Garner (Butterworths, London, 1957), pp. 68–75.

<sup>42</sup>Although H<sub>2</sub>O was not studied, this is a reasonable conclusion from the results with O<sub>2</sub> and CO<sub>2</sub> obtained by D. Brennan, D. O. Hayward, and B. M. W. Trapnell, *Proc. Phys. Soc. (London)* **A256**, 81 (1960); D. Brennan and F. H. Hayes, *Phil. Trans. Roy. Soc. London* **A258**, 347 (1965).

<sup>43</sup>J. A. Appelbaum and W. F. Brinkman, *Phys. Rev. B* **2**, 907 (1970).

<sup>44</sup>L. N. Lieberman, D. R. Fredkin, and H. B. Shore, *Phys. Rev. Letters* **22**, 539 (1969).

<sup>45</sup>C. A. Neugebauer, in *Structure and Properties of Thin Films*, edited by C. A. Neugebauer, J. B. Newkirk, and D. A. Vermilyea (Wiley, New York, 1959), pp. 358–369.

<sup>46</sup>C. Kittel, *Introduction to Solid State Physics* (Wiley,

New York, 1956), 2nd ed., Chap. 9, p. 219.

<sup>47</sup>D. C. Tsui, *Solid State Commun.* **7**, 91 (1969).

<sup>48</sup>J. A. Appelbaum, J. C. Phillips, and G. Tzouras, *Phys. Rev.* **160**, 554 (1967).

<sup>49</sup>U. Gradmann and J. Müller, *Phys. Status Solidi* **27**, 313 (1968).

<sup>50</sup>E. Grünbaum and R. Schwartz, *J. Appl. Phys.* **40**, 3364 (1969).

<sup>51</sup>V. M. Kosevich, L. S. Palatnik, and L. E. Chernyakova, *Fiz. Metal. i Metalloved.* **25**, 568 (1968) [*Phys. Metals Metallog.* **25**, 205 (1968)].

<sup>52</sup>C. A. Neugebauer, in *Physics of Thin Films II*, edited by George Hass and Rudolf E. Thun (Academic, New York, 1964), pp. 1–59; L. Holland, *Vacuum Deposition of Thin Films* (Chapman and Hall, London, 1963), pp. 205–208.

PHYSICAL REVIEW B

VOLUME 2, NUMBER 10

15 NOVEMBER 1970

## Anomalous Electron-Phonon Transport Properties of Impure Metals. I. The Electrical Resistivity

M. J. Rice

*General Electric Research and Development Center, Schenectady, New York 12301*

and

O. Bunce

*Parkhurst Institute, Isle of Wight, England*

(Received 2 January 1970)

The electron-phonon contribution  $\rho_{ep}(T, c)$  to the resistivity of an impure metal, or dilute metal alloy, can be drastically different from that of the ideally pure metal,  $\rho_{ep}^0(T)$ , if, in the region of the Fermi energy, the conduction-electron relaxation time  $\tau_0(\epsilon)$  for impurity scattering varies with energy  $\epsilon$  on a scale comparable to or less than the Debye energy  $\hbar\omega_D$  of the metal. This effect is a consequence of the sensitivity of the (inelastic) electron-phonon resistivity to any energy-dependent component in the nonequilibrium electron-distribution function. We present a working formula for the effect and indicate several important consequences for nontransitional metals containing magnetic or nonmagnetic transitional impurities. In the limit of small impurity concentrations  $c$ , the alloy and host electron-phonon resistivities are connected to the electron-diffusion thermopower  $S(T, c)$  of the alloy via the simple relation  $\rho_{ep}(T, c) \approx \rho_{ep}^0(T) \{1 + (\hbar\omega_D/\epsilon_F)^2 [S(T, c)/S_0(T)]^2\}$ , where  $S_0$  denotes the "free-electron" thermopower. More generally,  $\rho_{ep}(T, c)$ , and also  $\rho_{imp}(T, c)$ , the resistivity resulting from impurity scattering, are expressed in terms of the first and second derivatives of  $\tau_0$  at the Fermi energy  $\epsilon_F$ . The anomalous electron-phonon resistivity will cause sharp peaks to appear in the atomic-resistivity temperature curves of very dilute magnetic-impurity systems (e.g., CuFe, AuFe, AuMn). Experimentally, measurements of deviations from Matthiessen's rule should furnish useful information on the energy dependence of the electron-impurity scattering.

### I. INTRODUCTION AND SUMMARY

This paper is the first of a series of papers which deals with the influence of a very energy-dependent electron-impurity scattering cross section on the electron-phonon contributions to the electronic transport properties of an impure metal or dilute metal alloy. It is devoted to a discussion of the electrical resistivity.

Suppose a small concentration  $c$  of metallic im-

impurity atoms is dissolved in a pure metal. Let  $\rho_{ep}^0(T)$  denote the electron-phonon resistivity of the pure metal at temperature  $T$  and

$$\tau_0(\epsilon_F; c, T) = \tau_0(\epsilon_F),$$

the conduction-electron relaxation time which ensues for elastic scattering from the impurity atoms. We assume the presence of a single paramagnetic conduction band in which the energy of an electron